This article has been accepted for publication in a future issue of this journal, but has not been fully edited. Content may change prior to final publication. Citation information: DOI 10.1109/TIE.2020.3048317, IEEE Transactions on Industrial Electronics

A Comparative Study on Overall Efficiency of 2-Dimensional Wireless Power Transfer Systems Using Rotational and Directional Methods

Hanwei Wang, Cheng Zhang, *Member, IEEE*, Yun Yang, *Member, IEEE*, Hui Wen Rebecca Liang, *Student Member, IEEE* and Shu Yuen Ron Hui, *Fellow, IEEE*

***Abstract*-Two-dimensional (2-D) wireless power transfer (WPT) systems can be controlled by either the directional method or the rotational method. The rotational method refers to the use of omnidirectional transmitter generating rotational flux regardless of the load positions, while the directional method refers to the use of omnidirectional transmitter generating magnetic flux directly toward the power-consuming load directions. This paper compares the overall efficiency of the two methods for 2-D WPT systems. Theoretical analysis reveals that (i) the directional WPT can be more efficient than the rotational WPT with either single or multiple loads when the magnetic field vector is controlled within the feasible zones; (ii) the efficiency difference between the two methods are more significant when the dimensions of the receiver coils are smaller. Both simulation and experimental results are consistent in validating the two discoveries. They indicate that the averaged efficiency of the directional method is at least 5% higher than that of the rotational one.**

***Index Terms*—2-dimensional (2-D) wireless power transfer (WPT), rotational method, directional method.**

I. Introduction

Recent advancements have enabled wireless power transfer (WPT) to reach wide-spread commercialization stage with the success of the Qi standard launched in 2010 by the Wireless Power Consortium (WPC), now comprising over 550 companies worldwide [1]. Wireless charging pads for portable electronics such as mobile phones are not only available for domestic and office applications, they are also widely installed inside many new vehicles for charging mobile phones and other Qi-compatible devices. So far, most of the WPT applications based on near-field magnetic resonance [2] are of directional nature, meaning that the wireless power transmitters are designed to transmit wireless power directionally toward an area where the load with the receiver coil will be placed [3]-[6].

Omni-directional WPT systems have been reported in [7]-[16]. Among them, [7] has addressed an omnidirectional WPT system comprising a transmitter with 3 orthogonal coils and a receiver also with 3 orthogonal coils (Fig.1). In [7], several methods covering (i) periodic switching of the plane of rotation, (ii) frequency shift, (iii) single-axis amplitude modulation, (iv) double-axis amplitude modulation and (v) wide-band operation have been discussed for omnidirectional magnetic field generation. Based on the same orthogonal coils, [8] demonstrates that receiver coil can obtain wireless power at positions of multiple angles around the orthogonal transmitter structure. Reference [9] adopts 3 orthogonal-coil structures for both the transmitter and receiver module. However, an important principle has been pointed out in [10] and [11] that identical currents used in the orthogonal transmitter coils in [7]-[9] cannot generate magnetic flux vector in a true omnidirectional manner. Non-identical current control has to be used for true omnidirectional WPT systems [10], [11]. Non-identical current control has been further elaborated and generalized into a set of general control principle for detecting load positions and directing wireless power towards the loads in [12]. The general mathematical analyses of 2-D and 3-D WPT systems can be found in [13] and [14] respectively. A modified 3-transmitter-coil structure in the bowl or wok shape is reported in [15]. In order to develop load independent resonance for variable coupling situation in omnidirectional WPT systems, high-order resonant circuits are explored in [16]. High degree of spatial freedom for WPT can also be achieved with the use of large dipole structures [17]. In [18], receiver resonators are tuned at different frequencies so that the omnidirectional transmitter structure can select the load according to their respective tuned frequencies.

So far, limited literature has investigated the overall efficiency of omnidirectional WPT systems with the general control methods, i.e., the rotational method and the directional method. The rotational method is implemented by the phase angle modulation of transmitter currents and the generating magnetic field vector can rotate in a circle regardless of load positions [11]. The directional method is achieved by the amplitude modulation of transmitter currents and the generating magnetic field vector can point toward one direction

Manuscript received 6 Aug. 2020, revised 1 Nov. 2020,; accepted 19 Dec. 2020.

H. Wang is with the Department of Electrical and Computer Engineering, University of Illinois, Urbana-Champaign (hanweiw2@illinois.edu). Cheng Zhang is with the Department of Electrical and Electronic Engineering, University of Manchester, U.K. (cheng.zhang@manchester.ac.uk). Yun Yang is with the Department of Electrical Engineering, Hong Kong Polytechnic University, Hong Kong (yun1989.yang@polyu.edu.hk). H.W. Liang is with the Department of Electrical and Electronic Engineering, University of Hong Kong, Hong Kong (rebeccaliang0425@gmail.com). S.Y.R. Hui was with the University of Hong Kong and is now with the School of Electrical and Electronic Engineering, Nanyang Technological University (ron.hui@ntu.edu.sg) and Department of Electrical and Electronic Engineering, Imperial College London.

This article has been accepted for publication in a future issue of this journal, but has not been fully edited. Content may change prior to final publication. Citation information: DOI 10.1109/TIE.2020.3048317, IEEE Transactions on Industrial Electronics

according the positions of power consuming loads [12]. This paper bridges the research gap by comparing the overall efficiency of a 2-D WPT system with the two control methods. Practical results justify that the directional method can be more efficient than the rotational method when the magnetic field vector is controlled within the feasible zones, particularly when the receiver coil sizes become smaller.

II. Efficiency Analysis of 2-D WPT Systems

A. General Analysis of the System

A typical 2-D WPT system with multiple loads is depicted in Fig. 1. The transmitter (Tx) consists of two orthogonal coils, i.e., an *x*-axis coil (Coil-*x*) and a y-axis coil (Coil-y). The *N* numbers of receivers (Rx) are distributed around the Tx to pick up energy. Both the Tx and Rx are in series compensation to minimize the apparent power rating of the power supply and maximize the transfer capability, respectively,

$$\omega_o^2 = \frac{1}{L_{px}C_{px}} = \frac{1}{L_{py}C_{py}} = \frac{1}{L_{sn}C_{sn}} \quad (n = 1,2,\cdots,N) \quad (1)$$

where L_{px}, L_{py} and L_{sn} are the inductances of the Tx and Rx; C_{px}, C_{py} and C_{sn} are the compensated capacitances; ω_o is the resonant angular frequency.

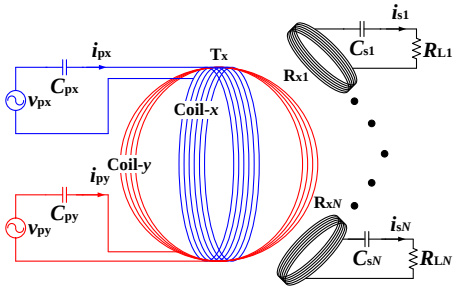

Fig. 1. Circuit diagram of a 2-D WPT system with multiple loads.

Based on the circuit diagram, the *M*-model of the circuitry in the frequency-domain can be given as

$$\begin{bmatrix}\mathbf{V_p}\\ \mathbf{O}\end{bmatrix} = \begin{bmatrix}\mathbf{Z_p} & -j\omega\mathbf{M_{TR}^T}\\ -j\omega\mathbf{M_{TR}} & \mathbf{Z_s}\end{bmatrix}\begin{bmatrix}\mathbf{I_p}\\ \mathbf{I_s}\end{bmatrix} \quad (2)$$

where $\mathbf{V_p} = \begin{bmatrix}v_{px}\\ v_{py}\end{bmatrix}$, $\mathbf{I_P} = \begin{bmatrix}i_{px}\\ i_{py}\end{bmatrix}$, $\mathbf{I_s} = \begin{bmatrix}i_{s1}\\ i_{s2}\\ \vdots\\ i_{sN}\end{bmatrix}$, $\mathbf{Z_p} = \begin{bmatrix}Z_{px} & 0\\ 0 & Z_{py}\end{bmatrix}$,

$$\mathbf{M_{TR}} = \begin{bmatrix}M_{xR1} & M_{yR1}\\ M_{xR2} & M_{yR2}\\ \vdots & \vdots\\ M_{xRN} & M_{yRN}\end{bmatrix},$$

$$\mathbf{Z_s} = \begin{bmatrix}Z_{s1} & j\omega M_{R1R2} & \cdots & j\omega M_{R1RN}\\ j\omega M_{R1R2} & Z_{s2} & \cdots & j\omega M_{R2RN}\\ \vdots & \vdots & \ddots & \vdots\\ j\omega M_{R1RN} & j\omega M_{R2RN} & \cdots & Z_{sN}\end{bmatrix},$$

$Z_{px} = j\omega L_{px} + \frac{1}{j\omega C_{px}} + r_{px}$, $Z_{py} = j\omega L_{py} + \frac{1}{j\omega C_{py}} + r_{py}$, $Z_{sn} = j\omega L_{sn} + \frac{1}{j\omega C_{sn}} + r_{sn} + R_{Ln}$ (n=1,2,…,N); v_{px}, v_{py}, i_{px} and i_{py} are the input voltages and currents of Tx; i_{sn} are the currents of Rx; r_{px}, r_{py} and r_{sn} are the equivalent series resistances (ESR) of Tx and Rx; R_{Ln} are the load resistances; M_{xRn} and M_{yRn} are the mutual inductances between Tx and Rx; M_{RnRm} (m=1,2,…,N, $m\neq n$) are the mutual inductances between Rx; ω is the operating angular frequency. Generally, the mutual inductances between Rx are negligible, i.e., M_{RnRm}=0 and the switching frequency is operated at the resonant frequency, i.e., ω=ω_o. Based on (2), the currents of Rx can be derived as

$$i_{sn} = \frac{j\omega_o M_{xRn} i_{px} + j\omega_o M_{yRn} i_{py}}{j\omega_o L_{sn} + \frac{1}{j\omega_o C_{sn}} + r_{sn} + R_{Ln}} \quad (n = 1,2,\cdots,N) \quad (3.1)$$

By substituting (1) into (3.1),

$$i_{sn} = \frac{j\omega_o M_{xRn} i_{px} + j\omega_o M_{yRn} i_{py}}{r_{sn} + R_{Ln}} \quad (n = 1,2,\cdots,N) \quad (3.2)$$

The total efficiency the 2-D WPT system is

$$\eta = \frac{\sum_{n=1}^{N} R_{Ln}|i_{sn}|^2}{\sum_{n=1}^{N} R_{Ln}|i_{sn}|^2 + r_{px}|i_{px}|^2 + r_{py}|i_{py}|^2} \quad (4)$$

By substituting (3.2) into (4),

$$\eta = \frac{\sum_{n=1}^{N} K_{1n}|i_{px}|^2 + K_{2n}|i_{py}|^2 + K_{3n} i_{px}\cdot i_{py}}{\sum_{n=1}^{N}(K_{1n}+r_{px})|i_{px}|^2 + (K_{2n}+r_{py})|i_{py}|^2 + K_{3n} i_{px}\cdot i_{py}} \quad (5)$$

where $K_{1n} = \frac{\omega_o^2 M_{xRn}^2 R_{Ln}}{(r_{sn}+R_{Ln})^2}$, $K_{2n} = \frac{\omega_o^2 M_{yRn}^2 R_{Ln}}{(r_{sn}+R_{Ln})^2}$ and $K_{3n} = \frac{2\omega_o^2 M_{xRn} M_{yRn} R_{Ln}}{(r_{sn}+R_{Ln})^2}$.

B. Efficiency of the System Using the Rotational Method

The resultant magnetic field vector of the 2-D WPT system can rotate in a circular manner (as shown in Fig. 2) by controlling the currents of Tx with the same magnitude I_m but 90° phase shift, i.e.,

$$\begin{cases} i_{px} = I_m e^{j\omega t} \\ i_{py} = I_m e^{j(\omega t + \frac{\pi}{2})} \end{cases} \quad (6)$$

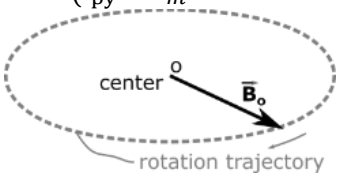

Fig. 2 A typical magnetic field vector of the 2-D WPT system using the rotational method.

This control method is called "rotational" method. The ability of rotating the magnetic field vector in a circular manner is equivalent to that of omnidirectional magnetic field vector in a 2-D sense. A receiving coil placed anywhere near the transmitter structure is able to pick-up a certain level of oscillating magnetic field.

By substituting (6) into (5), the overall efficiency of the 2-D WPT system controlled by the rotational method can be derived as

$$\eta_{rot} = \frac{\sum_{n=1}^{N} K_{1n} + K_{2n}}{\sum_{n=1}^{N} K_{1n} + K_{2n} + r_{px} + r_{py}} \quad (7)$$

C. Efficiency of the System Using the Directional Method

This article has been accepted for publication in a future issue of this journal, but has not been fully edited. Content may change prior to final publication. Citation information: DOI 10.1109/TIE.2020.3048317, IEEE Transactions on Industrial Electronics

The trajectory of the magnetic field vector of the 2-D WPT system can also form a straight line (as shown in Fig. 3) by controlling the currents of Tx in phase but different magnitudes, i.e.,

$$\begin{cases} i_{\mathrm{px}} = I_m \cos\theta e^{j\omega t} \\ i_{\mathrm{py}} = I_m \sin\theta e^{j\omega t} \end{cases} \tag{8}$$

where $\cos\theta$ and $\sin\theta$ are the amplitude modulation functions of i_{px} and i_{py}.

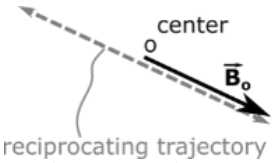

Fig. 3 A typical magnetic field vector of the 2-D WPT system using the directional method.

This control method is called "directional" method. By regulating the physical angle of the resultant magnetic field vector θ ($0°\le\theta<360°$), the current amplitudes of Tx can be theoretically controlled to reach any points in the space near the 2-D transmitting coil. When a single receiver coil is placed, the maximum efficiency of the WPT system can be achieved by controlling the central magnetic field to vertically penetrate the receiver coil plane.

By substituting (8) into (5), the overall efficiency of the 2-D WPT system controlled by the directional method can be derived as

$$\eta_{\mathrm{dir}} = \frac{\sum_{n=1}^{N} K_{1n}\cos^2\theta + K_{2n}\sin^2\theta + K_{3n}\sin\theta\cos\theta}{\sum_{n=1}^{N}(K_{1n}+r_{\mathrm{px}})\cos^2\theta + (K_{2n}+r_{\mathrm{py}})\sin^2\theta + K_{3n}\sin\theta\cos\theta} \tag{9}$$

D. Comparisons of the Two Methods

The efficiency difference between the two methods can be derived by subtracting (9) to (7), as given in (10.1), where

$$\Delta H = K_{4n}\sin 2\theta + K_{5n}\cos 2\theta \tag{10.2}$$

$$K_{4n} = \sum_{n=1}^{N} \frac{\omega_0^2 R_{\mathrm{L}n}}{(r_{\mathrm{s}n}+R_{\mathrm{L}n})^2} M_{\mathrm{xR}n} M_{\mathrm{yR}n} (r_{\mathrm{px}} + r_{\mathrm{py}}) \tag{10.3}$$

$$K_{5n} = \sum_{n=1}^{N} \frac{\omega_0^2 R_{\mathrm{L}n}}{(r_{\mathrm{s}n}+R_{\mathrm{L}n})^2} (r_{\mathrm{py}} M_{\mathrm{xR}n}^2 - r_{\mathrm{px}} M_{\mathrm{yR}n}^2) \tag{10.4}$$

In (10.2), if $K_{4n}>0$,

$$\Delta H = \sqrt{K_{4n}^2 + K_{5n}^2}\sin\left(2\theta + \tan^{-1}\frac{K_{5n}}{K_{4n}}\right) \tag{10.5}$$

If $K_{4n}<0$,

$$\Delta H = \sqrt{K_{4n}^2 + K_{5n}^2}\sin\left(2\theta + \tan^{-1}\frac{K_{5n}}{K_{4n}} + \pi\right) \tag{10.6}$$

where $-\frac{\pi}{2} < \tan^{-1}\frac{K_{5n}}{K_{4n}} < \frac{\pi}{2}$.

If $K_{4n}=0$,

$$\Delta H = K_{5n}\cos 2\theta \tag{10.7}$$

Based on (10.5), (10.6) and (10.7), the schematic diagram of the efficiency difference between the two methods can be depicted from the topic-view of the Tx, as shown in Fig. 4. When the magnetic field vector of the directional method is controlled in the feasible zones, the overall efficiency of the 2-D WPT system controlled by the directional method is higher than the rotational method.

For single Rx located in the typical 8 positions of 2-D WPT systems, as presented in Fig. 5, the efficiency difference of the two methods can be further derived based on (10.1), as given in (11.1). Here, to simplify the analysis without loss of generality, the ESR of coil-*x* and coil-*y* are assumed to be equal (i.e., $r_{\mathrm{px}}=r_{\mathrm{py}}=r_{\mathrm{p}}$) and the mutual inductances of the 8 cases are listed in Table I. Based on (11.1), the maximum and minimum efficiency differences (i.e., $\Delta\eta_{\max}$ and $\Delta\eta_{\min}$) can be derived by solving $\frac{\partial\Delta\eta}{\partial\theta}=0$. For all the 8 cases,

$$\Delta\eta_{\max} = \frac{\frac{\omega_0^2 M^2}{(r_{\mathrm{s}1}+R_{\mathrm{L}1})^2} R_{\mathrm{L}1} r_p}{\left[\frac{\omega_0^2 M^2}{(r_{\mathrm{s}1}+R_{\mathrm{L}1})^2} R_{\mathrm{L}1} + r_p\right]\left[\frac{\omega_0^2 M^2}{(r_{\mathrm{s}1}+R_{\mathrm{L}1})^2} R_{\mathrm{L}1} + 2r_p\right]} \tag{11.2}$$

$$\Delta\eta_{\min} = 0 \tag{11.3}$$

The corresponding phase angle of the directional method for achieving $\Delta\eta_{\max}$ and $\Delta\eta_{\min}$ are provided in Table I.

Based on (11.2), the plot of M^2-$\Delta\eta_{\max}$ can be depicted, as shown in Fig. 6. Here,

$$M_{\max} = \frac{\sqrt{2}(r_{\mathrm{s}1}+R_{\mathrm{L}1})^2 r_p}{\omega_0^2 R_{\mathrm{L}1}} \tag{12}$$

When the mutual inductance M equals to $M_{\max}$, $\Delta\eta_{\max}$ is maximized. For practical 2-D WPT systems, $M>M_{\max}$ always holds, which means a smaller M giving rise to a larger $\Delta\eta_{\max}$, and vice versa. For two Rx coils at the same position but with different sizes, due to the mutual inductance of the smaller Rx coil is smaller than that of the larger Rx coil, the advantages of gaining higher efficiency by the directional method is more prominent for the 2-D WPT system with single Rx.

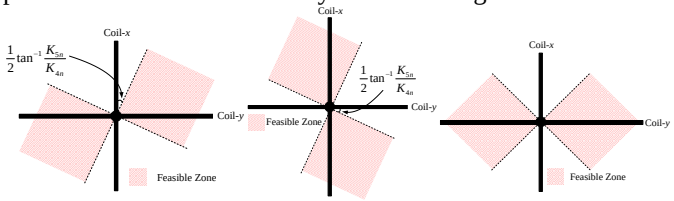

(a) $K_{4n}>0$ (b) $K_{4n}<0$ (c) $K_{4n}=0$

Fig. 4 Schematic diagram of the efficiency difference between the two methods.

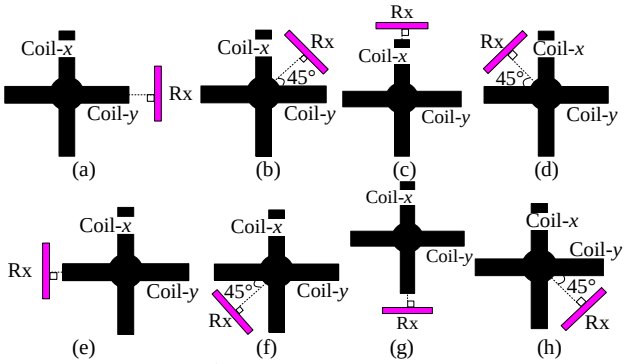

Fig. 5 Typical 8 positions of single Rx in the 2-D WPT system.

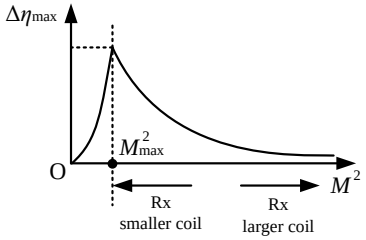

Fig. 6 plot of M^2-$\Delta\eta_{\max}$ based on the parameters of the 8-position cases

This article has been accepted for publication in a future issue of this journal, but has not been fully edited. Content may change prior to final publication. Citation information: DOI 10.1109/TIE.2020.3048317, IEEE Transactions on Industrial Electronics

$$\Delta\eta = \eta_{\mathrm{dir}} - \eta_{\mathrm{rot}} = \frac{\Delta H}{\left[\sum_{n=1}^{N}\left(K_{1n}+r_{\mathrm{px}}\right)\cos^2\theta+\left(K_{2n}+r_{\mathrm{py}}\right)\sin^2\theta+K_{3n}\sin\theta\cos\theta\right]\left[\sum_{n=1}^{N}K_{1n}+K_{2n}+r_{\mathrm{px}}+r_{\mathrm{py}}\right]} \tag{10.1}$$

$$\Delta\eta = \frac{\frac{\omega_0^2 R_{\mathrm{L1}} r_{\mathrm{p}}}{\left(r_{\mathrm{s1}}+R_{\mathrm{L1}}\right)^2}\left[\left(M_{\mathrm{xR1}}^2-M_{\mathrm{yR1}}^2\right)\cos 2\theta+2M_{\mathrm{xR1}}M_{\mathrm{yR1}}\sin 2\theta\right]}{\left[\frac{\omega_0^2 R_{\mathrm{L1}}}{\left(r_{\mathrm{s1}}+R_{\mathrm{L1}}\right)^2}\left(M_{\mathrm{xR1}}\cos\theta+M_{\mathrm{yR1}}\sin\theta\right)^2+r_{\mathrm{p}}\right]\left[\frac{\omega_0^2 R_{\mathrm{L1}}}{\left(r_{\mathrm{s1}}+R_{\mathrm{L1}}\right)^2}\left(M_{\mathrm{xR1}}^2+M_{\mathrm{yR1}}^2\right)+2r_{\mathrm{p}}\right]} \tag{11.1}$$

TABLE I. PARAMETERS OF THE 8-POSITION CASES

Positions	$(M_{\mathrm{xR1}}, M_{\mathrm{yR1}})$	$\Delta\eta_{\max}$	$\Delta\eta_{\min}$
Fig. 5(a)	$(M, 0)$	$\theta = 0$ or $\theta = \pi$	$\theta = \frac{\pi}{2}$ or $\theta = \frac{3\pi}{2}$
Fig. 5(b)	$\left(\frac{M}{\sqrt{2}}, \frac{M}{\sqrt{2}}\right)$	$\theta = \frac{\pi}{4}$ or $\theta = \frac{5\pi}{4}$	$\theta = \frac{3\pi}{4}$ or $\theta = \frac{7\pi}{4}$
Fig. 5(c)	$(0, M)$	$\theta = \frac{\pi}{2}$ or $\theta = \frac{3\pi}{2}$	$\theta = 0$ or $\theta = \pi$
Fig. 5(d)	$\left(-\frac{M}{\sqrt{2}}, \frac{M}{\sqrt{2}}\right)$	$\theta = \frac{3\pi}{4}$ or $\theta = \frac{7\pi}{4}$	$\theta = \frac{\pi}{4}$ or $\theta = \frac{5\pi}{4}$
Fig. 5(e)	$(-M, 0)$	$\theta = 0$ or $\theta = \pi$	$\theta = \frac{\pi}{2}$ or $\theta = \frac{3\pi}{2}$
Fig. 5(f)	$\left(-\frac{M}{\sqrt{2}}, -\frac{M}{\sqrt{2}}\right)$	$\theta = \frac{\pi}{4}$ or $\theta = \frac{5\pi}{4}$	$\theta = \frac{3\pi}{4}$ or $\theta = \frac{7\pi}{4}$
Fig. 5(g)	$(0, -M)$	$\theta = \frac{\pi}{2}$ or $\theta = \frac{3\pi}{2}$	$\theta = 0$ or $\theta = \pi$
Fig. 5(h)	$\left(\frac{M}{\sqrt{2}}, -\frac{M}{\sqrt{2}}\right)$	$\theta = \frac{3\pi}{4}$ or $\theta = \frac{7\pi}{4}$	$\theta = \frac{\pi}{4}$ or $\theta = \frac{5\pi}{4}$

IV. IMPLEMENTATION AND EVALUATION

Experiments are conducted based on the practical setup, the schematic of which is shown in Fig. 7. A photograph of the hardware setup is shown in Fig. 8. Only the x-axis and the y-axis of the 3-D transmitter are adopted to deliver power for the 2-D WPT system, while the z-axis of the 3-D transmitter remains open circuit. The high-frequency power supplies for both the x- and y-axis coils of the transmitting coil are implemented by the Tektronics AFG3102 Dual Channel Function Generator and the AR 25A250A RF power amplifier. The amplitude and the frequency of the sinusoidal signals provided by the function generator are controlled via the interface of Matlab in the PC. Both the x- and y-axis coils of the transmitting coil are constructed with Litz wires and have 11 turns. The diameters for both the x- and y-axis coils are 31 cm. *Rx* coils of two different diameters are used in the experiment. The large *Rx* coil has a diameter of 31cm while the small *Rx* coil has a diameter of 20 cm. The Rx coil resonator is loaded with a resistor of 3.24 Ω. The nominal parameters of the experiment setup are tabulated in Table II.

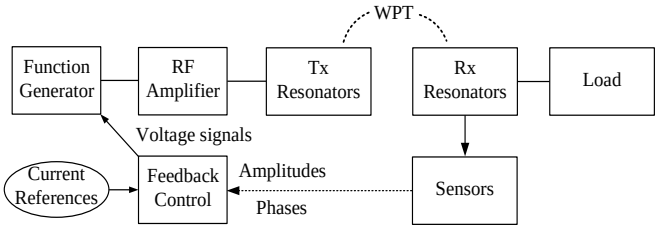

Fig. 7 Schematic of the experimental setup for the 2-D WPT system.

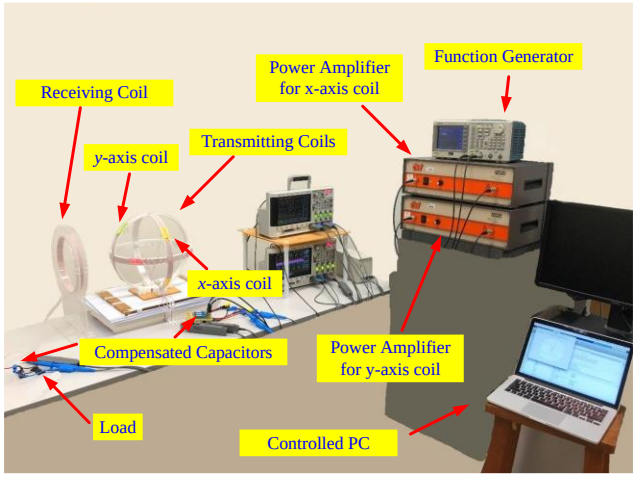

Fig. 8 A photograph of the practical setup.

TABLE II. PARAMETERS OF THE PRACTICAL SETUP

Parameter Name	Value
Transmitting coil diameter d_{Tx}	31 cm
Transmitting coil number of turns N_{Tx}	11
Transmitting coil inductance L_{Tx}	86.86 μH
Transmitting coil serial capacitance C_{Tx}	1 nF
Transmitting coil parasitic resistance R_{Tx}	1.61 Ω
Receiving coil diameter d_{Rx}	31 cm/20 cm
Receiving coil number of turns N_{Rx}	11
Receiving coil inductance L_{Rx}	86.35 μH/49.88 μH
Receiving coil serial capacitance C_{Rx}	1 nF/1.75 nF
Receiving coil parasitic resistance R_{Rx}	1.61 Ω/1.04 Ω
Load resistance R_{Load}	3.24 Ω
Power source frequency f	540 kHz

A. *Efficiency Comparisons of the Rotational and Directional WPT Methods for a Single Receiver*

For the 2-D WPT system with a single receiver, four cases are studied, as tabulated in Table III. The large Rx coil is adopted in cases 1 and 2, while the small Rx coil is adopted in cases 3 and 4. The load is placed in a range of angular locations with the *Rx* coil plane around and facing the center of the *Tx* structure at two fixed distances. The distance of 30 cm is adopted in cases 1 and 3, while the distance of 40 cm is adopted in cases 2 and 4. At each load location, the energy efficiency is obtained from the ratio of the load power and the input power of the transmitter. For the directional WPT tests, the two *Tx* coil currents will be programmed to generate a resultant magnetic field vector pointing directly towards the *Rx* coil center in each load location. The efficiency measurements taken with the *Rx*

This article has been accepted for publication in a future issue of this journal, but has not been fully edited. Content may change prior to final publication. Citation information: DOI 10.1109/TIE.2020.3048317, IEEE Transactions on Industrial Electronics

coil around the *Tx* structure over one cycle are expected to be the maximum efficiency point for that angular direction.

Note that the 2-D WPT system can be driven directly by power inverters. The power amplifiers are used only for convenience sake. The loss in the power source is therefore not considered in the comparison. The polar plot of the efficiency-angle curve for the case 1 is shown in Fig. 9 when the large *Rx* coil is placed at a distance of 30 cm from the center of the Tx structure. Here, the "solid" and "dashed" lines are the simulation results while the "triangle" and "circle" patterns are the practical measurements. It can be observed that the simulation results are highly consistent with the practical measurements for both methods. The directional WPT method achieves a higher efficiency than the rotational WPT method at any positions, which validates the analysis and the derived equations in (11). Therefore, it is reasonable to state that, in the case of a single load situation, the best approach is to do the scanning process, determine the load position and then zoom the wireless power towards the load directionally. This principle applies equally well even if the single load is placed further away from 30cm to 40cm as shown in Fig.10 for the case 2, although a longer transmission distance leads to a reduction in the energy efficiency. When putting the results of Figs. 9 and 10 in one polar plot, Fig. 11 show that the theoretical results are highly consistent with the practical measurements. Efficiency of directional and rotational method of two distances plotted in Cardioid coordinate and polar coordinate. The results confirm that the analysis is sufficiently accurate.

TABLE III. CASES INVESTIGATED FOR A SINGLE RECEIVER

Case	Rx coil diameter (cm)	Distance between Rx and Tx (cm)
1	31	30
2	31	40
3	20	30
4	20	40

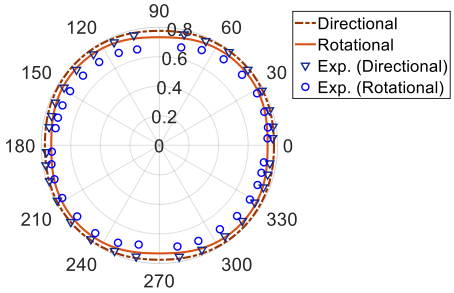

Fig. 9 Simulation and experimental efficiency curves of case 1.

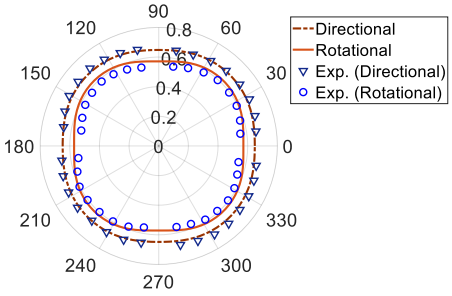

Fig. 10 Simulation and experimental efficiency curves of case 2.

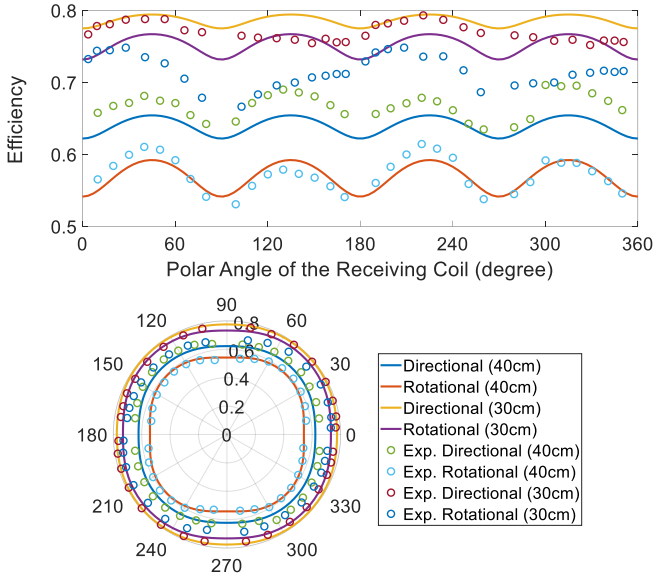

Fig. 11 Comparative results of cases 1 and 2 for the large Rx coil.

When the large Rx coil is replaced with the small counterpart with a diameter of 20 cm, the same sets of tests are repeated and the corresponding results are shown in Figs. 12 and 13. Obviously, a *Rx* coil with a small diameter has a lower efficiency than that of a large diameter for the same *Tx* structure. The reason is that a smaller coil will pick up less output power. Again, combining the results of Figs. 12 and 13 in one polar plot (Fig. 14) shows that the analysis is reliable and accurate. The efficiency measurements of directional and rotational method of two distances are plotted in Cardioid coordinate and polar coordinate. The efficiency differences of the two methods between the large *Rx* coil and small *Rx* coil are plotted in Fig. 15. Both simulation and experimental results confirm the analysis in Fig. 6 that the efficiency differences between the two methods are more significant for a smaller Rx coil.

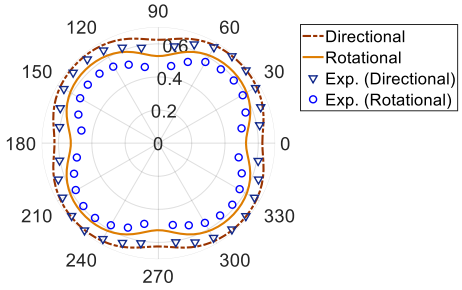

Fig. 12 Simulation and experimental efficiency curves of case 3.

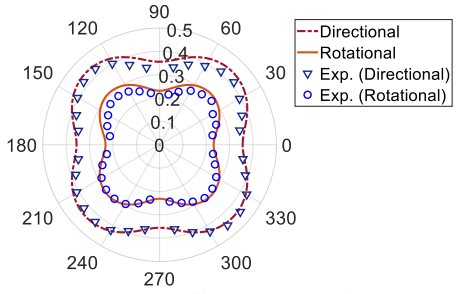

Fig. 13 Simulation and experimental efficiency curves of case 4.

This article has been accepted for publication in a future issue of this journal, but has not been fully edited. Content may change prior to final publication. Citation information: DOI 10.1109/TIE.2020.3048317, IEEE Transactions on Industrial Electronics

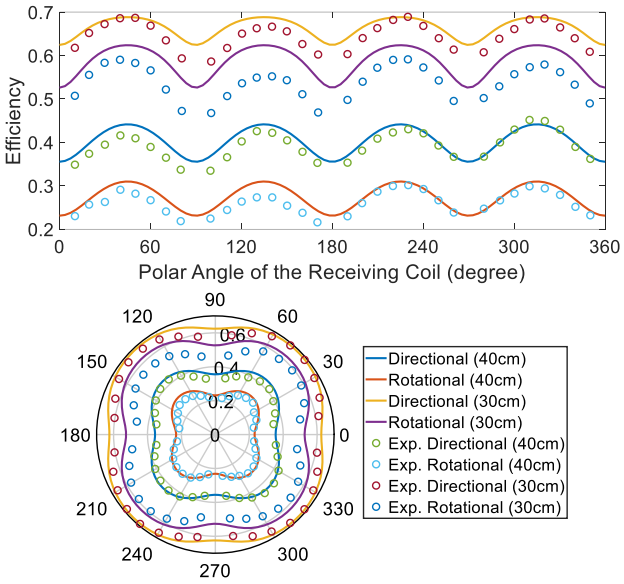

Fig. 14 Comparative results of cases 3 and 4 for the small Rx coil.

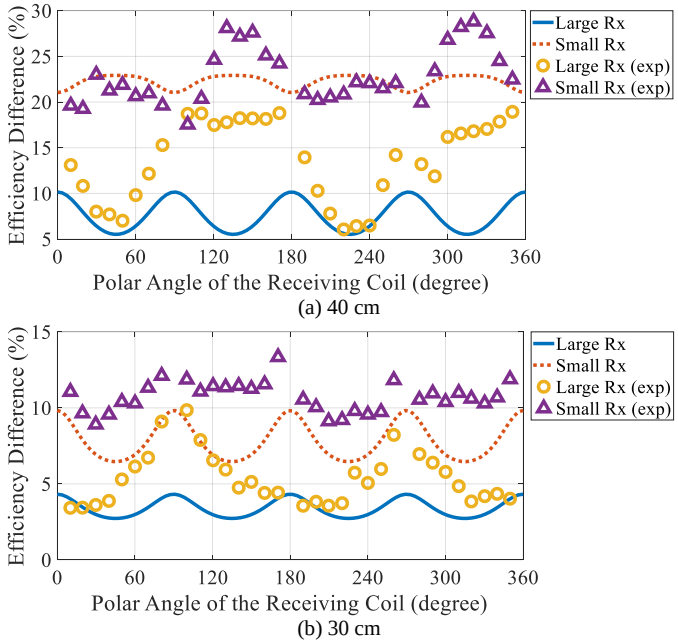

(a) 40 cm

(b) 30 cm

Fig. 15 Comparative results of efficiency differences between the large Rx coil and the small Rx coil.

B. *Efficiency Comparisons of the Rotational and Directional WPT Methods for Multiple Receivers*

For the 2-D WPT system with multiple receivers, twelve cases of WPT systems with two Rx coils (i.e., Rx-1 and Rx-2) are examined, as tabulated in Table IV. Both the parameters of small and large Rx coils are the same as the parameters given in Table II, while the load conditions are different. "Load-1" indicates the load connected to the Rx-1 and "Load-2" indicates the load connected to the Rx-1. "open" means no load is connected. The Rx coils are placed in two different sets of positions, as shown in Fig 16. The distance between the Tx and the Rx-1 or Rx-2 are fixed at 30 cm.

TABLE IV. CASES INVESTIGATED FOR MULTIPLE RECEIVERS

Case	Position	Rx-1	Rx-2	Load-1	Load-2
3	1	small	small	10 Ω	10 Ω
4	1	small	small	50 Ω	10 Ω
5	1	small	small	open	10 Ω
6	1	large	large	10 Ω	10 Ω
7	1	large	large	50 Ω	10 Ω
8	1	large	large	open	10 Ω
9	2	small	small	10 Ω	10 Ω
10	2	small	small	50 Ω	10 Ω
11	2	small	small	open	10 Ω
12	2	large	large	10 Ω	10 Ω
13	2	large	large	50 Ω	10 Ω
14	2	large	large	open	10 Ω

For the rotational method, due to the two receivers are placed in fixed positions, the overall efficiency of the loads almost remains constant for each case. The overall efficiencies of the rotational WPT for the twelve cases in both simulation and experiment are provided in Table V.

For the directional method, the currents supplied to the transmitter coils are in-phase and the current vector is rotated in discrete angular steps. The ratio of each load power and the total input power over one cycle can be measured and plotted (plots for the cases 3, 4 and 5 are presented in Fig. 17). Based on power efficiency of each load, the overall efficiencies of the directional method can be further plotted (plots for the cases 3, 4 and 5 are presented in Fig. 18). The directional method can search out and control the 2-D WPT system operating at the maximum efficiencies, which are listed in Table V.

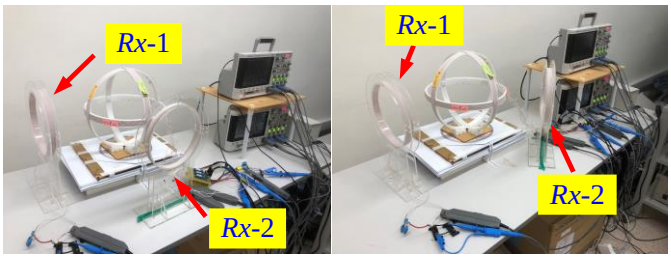

(a) position-1 (b) position-2

Fig. 16 Experimental setup of the 2-D transmitter structure with two receiver loads at the position-1 and position-2.

The overall efficiencies of all the twelve cases in Table V are depicted in Fig. 19. In both simulation and experiment results, the directional method exhibits higher efficiency than the rotational method for all the cases with different Rx coil positions, Rx coil sizes and load impedances, which validates the analysis and the derived equations in (11). Besides, the efficiencies between the small Rx coils and the large Rx coils are presented in Fig. 20. The results show that the large Rx coils can harvest more energy than the small Rx coils for both rotational and directional methods when the load conditions are the same. The efficiency differences of the two methods between the large Rx coil and small Rx coil are plotted in Fig.

This article has been accepted for publication in a future issue of this journal, but has not been fully edited. Content may change prior to final publication. Citation information: DOI 10.1109/TIE.2020.3048317, IEEE Transactions on Industrial Electronics

21. Apparently, the efficiency differences between the two methods are more significant for small Rx coils, which validates the analysis in Fig. 6. The averaged efficiencies of the rotational and directional methods are also calcuated and shown in Table V. It is noted that the averaged efficiency of the directional method is 5% higher than that of the rotational counterpart. This result confirms the advantage of the directional WPT approach.

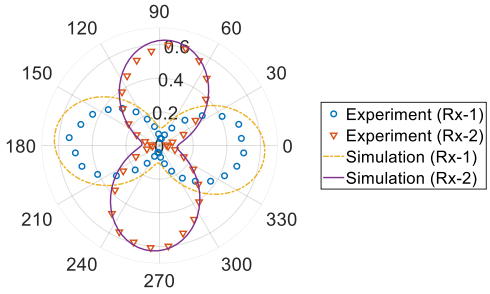

(a) case 3

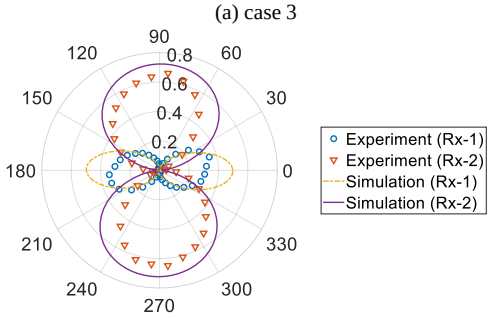

(b) case 4

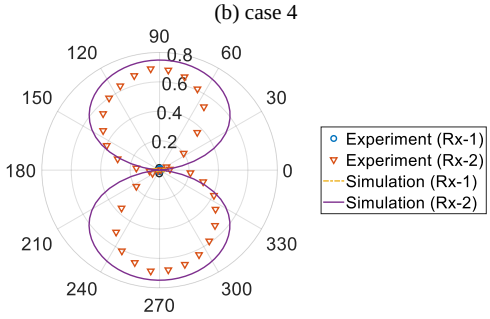

(c) case 5

Fig. 17 Power polar plot of the directional WPT for the cases 3, 4 and 5.

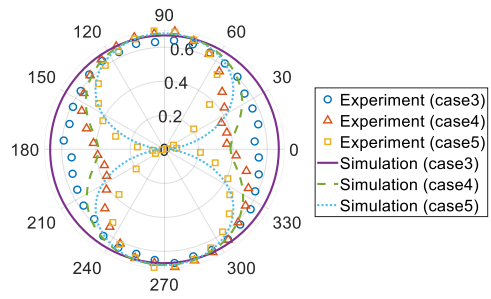

Fig. 18 Overall efficiency of the directional WPT for the cases 3,4 and 5.

TABLE V. OVERALL EFFICIENCY FOR MULTIPLE RECEIVERS

Case	Method	Simulation	Experiment
3	Rotational	62.55%	59.72%
	Directional	66.97%	64.16%
4	Rotational	60.34%	57.93%
	Directional	68.93%	67.04%
5	Rotational	58.78%	55.11%
	Directional	69.06%	68.22%
6	Rotational	76.01%	73.97%
	Directional	78.81%	75.95%
7	Rotational	70.14%	68.4%
	Directional	73.31%	71.21%
8	Rotational	66.68%	62.56%
	Directional	70.83%	69.09%
9	Rotational	62.01%	57.77%
	Directional	66.98%	61.07%
10	Rotational	62.27%	59.22%
	Directional	69.16%	64.17%
11	Rotational	61.17%	55.34%
	Directional	70.32%	65.11%
12	Rotational	78.11%	75.99%
	Directional	80.24%	78.28%
13	Rotational	76.61%	74.57%
	Directional	79.4%	78.21%
14	Rotational	73.71%	72.19%
	Directional	79.39%	79.36%
	Rotational Average (RAv)	**67.37%**	**64.40%**
	Directional Average (DAv)	**72.78%**	**70.16%**
	Efficiency Improvement of the Direactional Method (DAv – RAv)	**5.41%**	**5.76%**

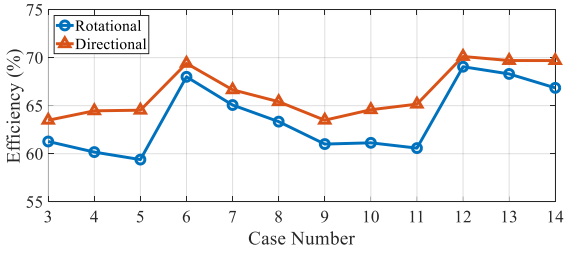

(a) simulation

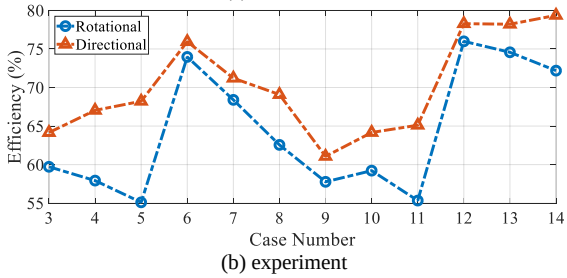

(b) experiment

Fig. 19 Comparative results of efficiency between the two methods for multiple receivers.

This article has been accepted for publication in a future issue of this journal, but has not been fully edited. Content may change prior to final publication. Citation information: DOI 10.1109/TIE.2020.3048317, IEEE Transactions on Industrial Electronics

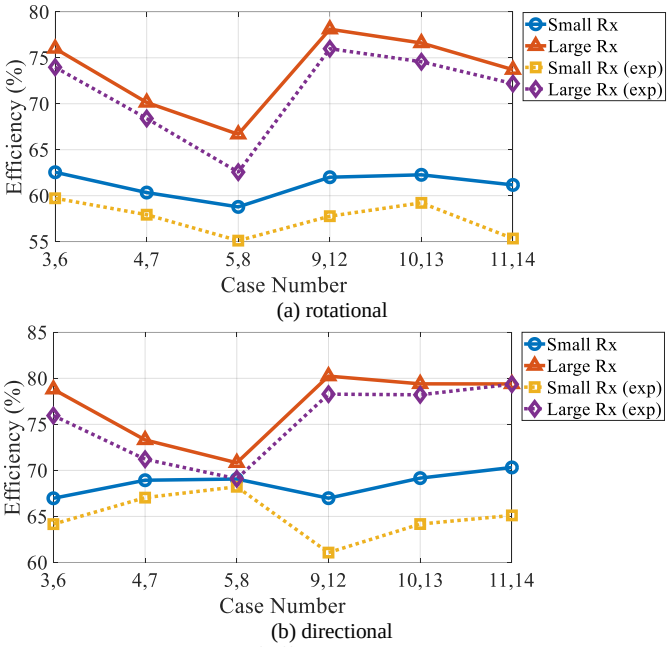

Fig. 20 Comparative results of efficiency between the small Rx coils and the large Rx coils.

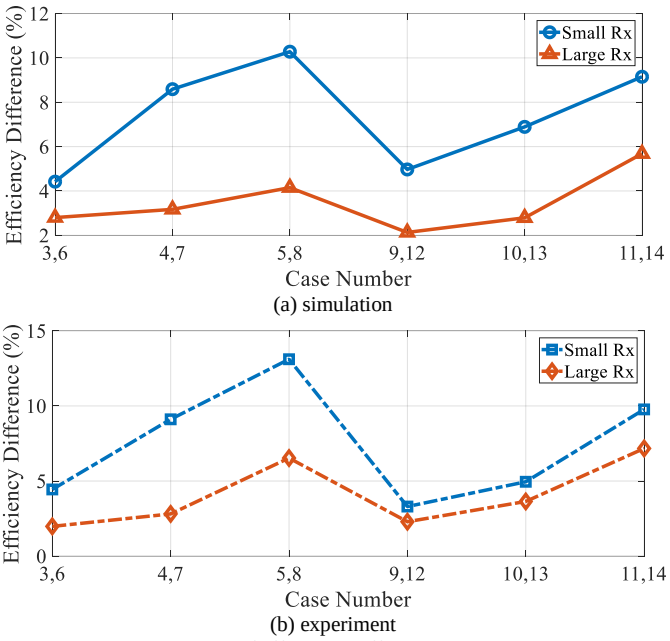

Fig. 21 Comparative results of efficiency difference between the large Rx coils and the small Rx coils.

V. Conclusions

This paper presents a comparative study on the rotational and directional WPT methods for 2-D WPT systems. The directional WPT method presumes the knowledge of load position identification via scanning the power delivered in discrete steps over a cycle so that the transmitter coil currents are controlled to point the resultant magnetic field vector directly towards the loads. The rotational method simply controls the two transmitter coil currents to rotate the magnetic field vector at high resonant frequency regardless of the locations of the loads. For the first time, a mathematical proof has been developed to show that the directional WPT approach is more efficient than the rotational WPT approach, particularly when the receiver coil sizes become smaller (a situation in which the directional WPT approach is more effective). These findings have been confirmed with both theoretical analysis and practical measurements. The results obtained in the experimental setup confirm that the energy efficiency of the directional method is at least 5% higher than that of the rotational method. Efficiency improvement of the directional WPT method increases with the dimension differences between the transmitter and receiver coils. The results in this study lead to the following important conclusion. Omnidirectional WPT should preferrably adopt the strategy of using the rotational WPT method to scan the power absorption at different angles in order to locate the load positions and then use the directional WPT method to focus the wireless power towards the loads for improved performance.

References

[1] [online] Wireless power consortium: https://www.wirelesspowerconsortium.com, October 2018

[2] S.Y.R. Hui, ""Magnetic Resonance for Wireless Power Transfer [A Look Back], IEEE Power Electronics Magazine, Vol. 3, Issue:1, 2016, pp: 14-31

[3] G.A. Covic and J. T. Boys, "Inductive power transfer", Proceedings of the IEEE, Vol. 101, No.6, June 2013, pp: 1276-1289

[4] J.S. Ho, S. Kim and A.S.Y. Poon, "Midfield wireless powering for implantable systems", Proceedings of the IEEE, Vol. 101, No.6, June 2013, pp: 1369-1378

[5] C. Mi, G. Buja, S. Choi; C.. Rim, "Modern Advances in Wireless Power TransferSystems for Roadway Powered Electric Vehicles", IEEE Transactions on Industrial Electronics, 2016, Volume: 63, Issue: 10, Pages: 6533 – 6545

[6] S.. Hui, "Planar wireless charging technology for portable electronic produts and Qi", Proceedings of the IEEE, Vol. 101, No.6, June 2013, pp: 1290-1301

[7] Kthleen O'Brien, "Inductively coupled radio frequency power transmission system for wireless systems and devices", Ph.D thesis, Technische Universitat Dresden, May 2006, Chapter 3 – Chapter 4, pp: 33-84

[8] D. Wang, Y. Zhu, Z. Zhu, T.T. Mo and Q. Huang, "Enabling multi-angle wireless power transmission via magnetic resonant coupling", International Conference on Computing and Convergence Technology (ICCCT) 2012, pp: 1395-1400

[9] O. Jonah, S.V. Georgakopoulos and M.M. Tentzeris, "Orientation insensitive power transfer by magnetic resonance for mobile devices", IEEE Wireless Power Transfer, Perugia, Italy, 15-16 May 2013, pp:5-8.

[10] W. M. Ng, C. Zhang, D. Lin and S. Y. Ron Hui, "Two- and Three-Dimensional Omnidirectional Wireless Power Transfer," in *IEEE Transactions on Power Electronics*, vol. 29, no. 9, pp. 4470-4474, Sept. 2014.

[11] W. M. Ng C. Zhang D. Lin S. Y. R. Hui "Omni-directional wireless power transfer systems," U.S. Patent Application, Application No. 13/975,40, Aug. 26, 2013.

[12] Zhang C., Lin Deyan and Hui S.Y.R., "Basic Control Principles of Omnidirectional Wireless Power Transfer", IEEE Transactions on Power Electronics, Vol.31, No.7, July 2016, pages: 5215-5227.

[13] D. Lin, C. Zhang and S. Y. R. Hui, "Mathematical Analysis of Omnidirectional Wireless Power Transfer—Part-I: Two-Dimensional Systems," in *IEEE Transactions on Power Electronics*, vol. 32, no. 1, pp. 625-633, Jan. 2017.

[14] D. Lin, C. Zhang and S. Y. R. Hui, "Mathematic Analysis of Omnidirectional Wireless Power Transfer: Part-II Three-Dimensional Systems", IEEE Transactions on Power Electronics, Vol.32, Issue 1, 2017, pp: 613-624

[15] J. Feng ; Q. Li ; F.C. Lee, “Omnidirectional wireless power transfer for portable devices”, 2017 IEEE Applied Power Electronics Conference and Exposition (APEC), Pages: 1675 – 1681
[16] J. Feng ; M. Fu ; Q. Li ; F. C. Lee, “Resonant converter with coupling and load independent resonance for omnidirectional wireless power transfer application”, 2017 IEEE Energy Conversion Congress and Exposition (ECCE), Pages: 2596 – 2601
[17] Bo H. Choi ; Eun S. Lee ; Yeong H. Sohn ; Gi C. Jang ; Chun T. Rim, “Six Degrees of Freedom Mobile Inductive Power Transfer by Crossed Dipole Tx and Rx Coils”, IEEE Transactions on Power Electronics, 2016, Volume: 31, Issue: 4, Pages: 3252 – 3272
[18] Z. Dai ; Z. Fang ; H. Huang ; Y. He ; J. Wang, “Selective Omnidirectional Magnetic Resonant Coupling Wireless Power Transfer With Multiple-Receiver System”, IEEE Access,2018, Volume: 6, Pages: 19287 – 19294

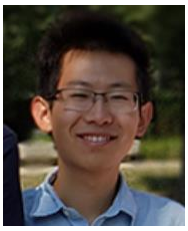

Hanwei Wang received his B.Sc. degree from the Department of Physics at Tsinghua University, Beijing, China, in 2019. He is currently pursuing Ph.D. degree at Department of Electrical and Computer Engineering at University of Illinois at Urbana-Champaign (UIUC). He is interested in developing artificial electromagnetic materials’ applications in biomedical imaging and Bio-sensors. His research interests include metamaterials, optical force microscopy, magnetic resonance imaging and wireless power transfer.

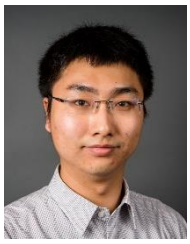

Cheng Zhang (S’13–M’16) was born in China, in 1990. He received the B.Eng. degree (first class Hons.) in electronic and communication engineering from the City University of Hong Kong, Hong Kong, in 2012 and the Ph.D. degree in electronic and electrical engineering from The University of Hong Kong, Hong Kong, in 2016.

From 2016 to 2017, he was a Senior Research Assistant in the Department of Electrical and Electronic Engineering, The University of Hong Kong. He was a Postdoctoral Research Associate in the Research Laboratory of Electronics, Massachusetts Institute of Technology, Cambridge, MA, USA from 2017 to 2018. He is now working at the University of Manchester as a lecturer in power electronics. His research interests include high-frequency ac–dc power conversions and designs and optimizations for wireless power transfer applications.

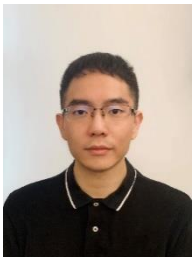

Yun Yang (S’13-M’18) received his B.Sc. degree in Electrical Engineering from Wuhan University in 2012 and Ph.D. degree in Electrical Engineering from The University of Hong Kong in 2017. He then became a Postdoctoral-Fellow in the same research group. Now, he is a Research Assistant Professor in the Department of Electrical Engineering, the Hong Kong Polytechnic University and an Honorary Research Assistant Professor in the Department of Electrical and Electronic Engineering, the University of Hong Kong. He has authored or coauthored more than 40 technical papers, including 10 leading journals published as the first author. He also has two book chapters and two U.S. patent applications. His research interests include wireless power transfer, microgrid, power electronics and control.

H. W. Rebecca Liang received her B.S. and M.S. degrees in Electrical and Electronic Engineering from National Cheng Kung University, Taiwan in 2013 and 2015, respectively. In 2015-2017, she worked as an analog circuit engineer at Chroma ATE (Advanced Technology Research Center), Taiwan. She is currently working towards a PhD at the University of Hong Kong. Her research interests include power electronics, wireless power transfer, dc-dc power converter, and renewable energy conversion.

S. Y. (Ron) Hui (M’87-SM’94-F’03) received his BSc (Eng) Hons in Electrical and Electronic Engineering at the University of Birmingham in 1984 and a D.I.C. and PhD in Electrical Engineering at Imperial College London in 1987. Previously, he held academic positions at the University of Nottingham and University of Sydney. In 2011-2021, he was the Philip Wong Wilson Wong Chair Professor at the University of Hong Kong. Presently, he holds the MediaTek Professorship at Nanyang Technological University and Chair Professorship of Power Electronics at Imperial College London.

He has published over 450 research papers including 300 refereed journal publications. Over 60 of his patents have been adopted by industry worldwide. His research interests include power electronics, wireless power, sustainable lighting and smart grid. His inventions on wireless charging platform technology underpin key dimensions of Qi, the world's first wireless power standard, with freedom of positioning and localized charging features for wireless charging of consumer electronics. He also developed the Photo-Electro-Thermal Theory for LED Systems. He received the IEEE Rudolf Chope R&D Award and the IET Achievement Medal (The Crompton Medal) in 2010 and IEEE William E. Newell Power Electronics Award in 2015. He is a Fellow of the Australian Academy of Technology & Engineering, US National Academy of Inventors and Royal Academy of Engineering, U.K.